Aerospace Science and Technology 46 (2015) 374–385

Contents lists available at ScienceDirect

Aerospace Science and Technology

www.elsevier.com/locate/aescte

Analytic approach to determine optimal conditions for maximizing altitude of sounding rocket: Flight in standard atmosphere

Sang-Hyeon Lee [a,*,1], Ralph C. Aldredge [b,2]

[a] Dept. of Mechanical Eng., University of Ulsan, Ulsan, 680-749, Republic of Korea
[b] Dept. of Mechanical and Aerospace Eng., University of California, Davis, CA, 95616, USA

ARTICLE INFO

Article history:
Received 21 November 2014
Received in revised form 5 August 2015
Accepted 16 August 2015
Available online 18 August 2015

ABSTRACT

The analytic approach to determine the optimal conditions for maximizing altitude of a sounding rocket is extended to the case in which the rocket flies in a standard atmosphere where the air density as well as the gravitational acceleration changes with altitude. The one-dimensional rocket momentum equation including thrust, gravitational force, and aerodynamic drag is solved. Flight in the standard atmosphere is analyzed by dividing the whole flight time into small intervals where the drag parameter and gravitational acceleration can be treated as constant in each interval. The analytic approach gives piecewise exact solutions of the rocket velocity and altitude that agree well with the numerical ones. A characteristic equation exists and provides accurate predictions of the optimal conditions for maximizing altitude at burn-out state or apogee.

1. Introduction

Scientific studies with a sounding rocket are simple, fast, and inexpensive compared to those with a satellite. The costs for a sounding rocket mission are much lower than those required for an orbiter mission, since sounding rocket missions do not need expensive boosters, extended telemetry or tracking coverage. Mission costs are also low because of the acceptance of a higher degree of risk in the mission compared to orbital missions [1]. Many countries are running sounding rocket programs and trying to develop technologies related to sounding rockets to exploit these advantages [2–13]. Most scientific measurements, observations, or experiments for sounding rocket missions are carried out near apogee. The low speed near apogee provides favorable chances to explore or observe space in a short time period. Furthermore, there are some important regions of space that are too low to be sampled by satellites; thus, sounding rockets provide platforms to carry out in-situ measurements in these regions [10]. Some microgravity environments [14,15] are carried after burn-out state and some scramjet experiments [16,17] are conducted during free-fall that provides a good hypersonic condition at low cost.

We consider the motion of a sounding rocket launched in the vertical direction for simplicity. Then the motion of a sounding rocket can be described with a one-dimensional momentum equation that includes thrust, gravitational force, and aerodynamic drag force. The rocket mass varies with time, and the aerodynamic drag is proportional to the square of the rocket velocity, which makes the governing equation nonlinear. Thus, we cannot obtain analytic solution in a general form. Hence, in most cases, numerical approaches are used to obtain solutions because of easy implementation with less assumption. An approximate solution can be obtained with neglecting drag force but it contains serious errors especially near ground. There are also approximate solutions with the Taylor series expansion, the perturbation method or the least square method [18], but they are complex and do not give information about the optimal conditions. Analytic solutions, on the contrary to numerical ones, are exact without numerical errors, give insights to understand the behavior of the system, show critical parameters, and lead to ways to determine the optimal conditions. Therefore it is necessary to obtain analytic solutions if possible.

An analytic exact solution of the rocket equation including aerodynamic drag exists only in a typical situation where all the forces are well balanced [19]. As a beginning study, we consider the typical case where an analytic solution exists. We are aware that the

* Corresponding author.
E-mail addresses: lsh@mail.ulsan.ac.kr (S.-H. Lee), rcaldredge@ucdavis.edu (R.C. Aldredge).
[1] Professor, (Aerospace Div.).
[2] Professor.

http://dx.doi.org/10.1016/j.ast.2015.08.004
1270-9638/

Nomenclature

D	drag
F	thrust
G	ratio between inertia and drag
g	gravitational acceleration
h	altitude
K	drag parameter
m	rocket mass
$\dot{m}$	rate of rocket mass change or mass flow rate of propellant jet
q	velocity parameter for rocket velocity
t	time
u	velocity of propellant jet
v	rocket vertical velocity
p	static pressure
T	temperature
ρ	density
Ω	rocket mass ratio between total mass and dry mass
ω	rocket mass ratio between adjacent intervals

Subscripts

a	ambient air
b	burn-out state
e	jet condition at rocket nozzle exit
o	ground state
opt	optimal condition for maximizing altitude
s	stationary state (apogee)

present approach could not be directly applied to the real cases. For instance, most of sounding rockets are designed to maintain the combustion chamber pressure to be constant for stable and safe operations, which lead to the constant mass flow of propellant. We could not make an analytic approach to the cases since there are no analytic solutions of the rocket momentum equation. However the present analytic approach could be useful to build a method to obtain a pseudo-analytic or an approximate solution.

The design target of a sounding rocket is the altitude at burn-out state or apogee. The rocket altitude can be changed with the ejection conditions of the propellant jet. Therefore, it is necessary to determine an optimal condition for maximizing altitude at given launching conditions. The Goddard problem of the optimal thrust programming for maximizing altitude of a rocket in vertical flight has been extensively studied with variation methods, asymptotic approach or optimal control theory [20–23]. But they are not based on the analytic solution of the rocket momentum equation. The previous study [19] showed an analytic approach to obtain exact solution of the rocket equation and to determine optimal condition for maximizing altitude. However the previous study cannot be applied to a sounding rocket flying in a real atmosphere where the air density changes with altitude. The objective of the present study is to extend the analytic approach to the flight in a real situation.

In a real atmosphere, even in calm conditions without wind, the air density dramatically changes with altitude, location or time. Also the gravitational acceleration cannot be treated as a constant when rockets go up to the upper atmosphere. Moreover, aerodynamic drag coefficient changes with the flight Mach number especially around the Mach number of unity. Hence aerodynamic drag is variable with altitude or rocket velocity. These make it impossible to obtain an analytic solution of the governing equation valid through the whole flight time. Therefore, we have to change the strategy to approach the problem. A “divide-and-conquer” strategy could be an alternative to avoid the serious problems. We can divide the whole flight time into intervals small enough to treat the air density, the gravitational acceleration and drag coefficient as constants in each interval. We can then have piecewise analytic solutions and also determine the optimal conditions.

The rocket considered in the present study is a simplified model based the Korea Sounding Rocket Program (KSR II and III). KSR II is a solid propellant rocket with total the weight of 2.0 ton, the diameter of 0.42 m and the length of 11.0 m. KSR III is a liquid propellant rocket with the weight of 6.1 ton, the diameter of 1.0 m and the length of 13.5 m. In the present study, we consider the medium specification between KSR II and KSR III.

2. One-dimensional rocket equation

2.1. Equation in boost phase

The motion of a sounding rocket in boost phase climbing in the vertical direction can be described with the following one-dimensional rocket equation [24,25].

$$m\frac{dv}{dt} = F - D - mg. \tag{2.1}$$

The mass of a rocket decreases with the mass flow of propellant.

$$m = m_o + \int_o^t \dot{m}dt, \tag{2.2a}$$

$$\dot{m} = \frac{dm}{dt}. \tag{2.2b}$$

The mass flow rate $\dot{m}$ is equal to the rate of rocket mass and has a negative sign by definition.

The thrust F is composed of two parts:

$$F = \dot{m}u_e + A_e(p_e - p_a). \tag{2.3}$$

For an adiabatic nozzle flow, the total enthalpy is constant, and then we can assume that the jet velocity u_e is constant. The jet velocity has the negative sign since its direction is opposite to the rocket velocity; thus, the thrust term $\dot{m}u_e$ has the positive sign. If the nozzle flow has a perfect expansion, the second term of the thrust vanishes. Hereafter, we ignore the second term of the thrust for simplicity.

The aerodynamic drag force D that proportional to the square of rocket velocity can be represented as follows:

$$D = Kv^2, \tag{2.4a}$$

$$K = \frac{S}{2}C_d\rho_a. \tag{2.4b}$$

The terms S and C_d are the cross-sectional area of a rocket and the aerodynamic drag coefficient, respectively. The air density of a standard atmosphere is not a constant but changes with altitude, which means that the drag parameter K also changes with altitude. The aerodynamic drag coefficient is usually increases sharply near the Mach number of unity and decreases gradually with the Mach number after then [18,26,27]. Some preliminary numerical experiments showed that this model caused serious numerical oscillations especially when the velocity parameter is near to speed of sound, which seems due to the abrupt change of the drag coefficient around the Mach number of unity. We adopt a modified

model to guarantee smooth changes of the drag coefficient at all Mach numbers. The details will be presented in Section 5.2.

The change of the gravitational force due to the altitude change should be considered for high altitude sounding rockets. In the present study, the following relation is used.

$$g = g_o \frac{R_E^2}{(R_E + h)^2}. \tag{2.4c}$$

The terms g_o and R_E stand for the gravitational acceleration and average radius of the earth at sea level that are 9.8067 (m/s^2) and 6.371×10^6 (m), respectively.

The governing equation then becomes

$$m\frac{dv}{dt} = \dot{m}u_e - Kv^2 - mg. \tag{2.5}$$

The mass is variable with time, and the square of the solution appears in the drag force, which makes the governing equation nonlinear. Thus, we could not obtain analytic solutions in a general form. However, there is a typical case where an analytic solution exists. We introduce a velocity parameter as follows:

$$q = \sqrt{\frac{\dot{m}u_e - mg}{K}}. \tag{2.6a}$$

The governing equation can then be reduced as

$$m\frac{dv}{dt} = K\left(q^2 - v^2\right). \tag{2.6b}$$

Separating variables leads to

$$\frac{dv}{q^2 - v^2} = \frac{K}{m}dt. \tag{2.6c}$$

This governing equation can be represented according to the mass instead of the time as follows:

$$\frac{dv}{q^2 - v^2} = \frac{K}{m}\frac{dm}{\dot{m}}. \tag{2.7}$$

We can obtain an analytic integration of the left hand side of the above equation only when the velocity parameter is constant. If the velocity parameter is constant, the mass flow rate is not a constant since the velocity parameter is constant. For a saturated gaseous nozzle flow the mass flow rate changes proportionally to the throat area or the chamber pressure. It is technically difficult to change the nozzle shape. Thus it is better to control the mass flow rate by the pressure of the rocket combustor. On the other hand, if the mass flow rate is constant, the velocity parameter becomes a function of mass and thus the left hand side of the above equation cannot be analytically integrated. Then, in this case, we should try to obtain an approximate solution.

Even though the left hand side can be analytically integrated, on the contrary to the previous study [23], the right hand side cannot be analytically integrated over the whole flight time since the drag parameter changes with the altitude or the Mach number and thus could not expressed as an explicit function of the time or the mass. Hence we could not obtain analytic solutions valid throughout the whole flight time. Then we have to find out another way to avoid such serious difficulties. This will be discussed in the next section.

2.2. Equation in coast phase

After the propellant of a rocket is totally consumed, the flight phase turns into coast phase, where the rocket climbs with inert force until the stationary state or apogee. The rocket equation becomes then

$$m_b\frac{dv}{dt} = -Kv^2 - m_b g. \tag{2.8a}$$

Separating variables yields

$$\frac{dv}{Kv^2 + m_b g} = -\frac{1}{m_b}dt, \quad \text{or} \tag{2.8b}$$

$$\frac{vdv}{Kv^2 + m_b g} = -\frac{1}{m_b}dh. \tag{2.8c}$$

An analytic solution of the above equation can be obtained if and only if the drag parameter is constant. As mentioned in equation (2.6c), we could not obtain analytic solutions valid throughout whole flight time since the drag parameter cannot be expressed as an explicit function of the velocity. This will be discussed in detail in the next section.

3. Analytic solutions

3.1. Solutions of the governing equation

3.1.1. Solutions in boost phase

The mass flow rate for a constant velocity parameter is variable with the mass and the drag parameter as follows:

$$\dot{m} = \frac{mg + Kq^2}{u_e}. \tag{3.1.1}$$

Inserting this relation into the governing equation yields

$$\frac{dv}{q^2 - v^2} = \frac{Ku_e}{mg + Kq^2}\frac{dm}{m}. \tag{3.1.2}$$

In the standard atmosphere, the air density and thus the drag parameter change with altitude even though the aerodynamic drag coefficient is constant. If the drag parameter is a function of altitude and so is the gravitational acceleration, then we cannot have a valid solution over the whole flight time. We then have to change the strategy to approach the problem. A divide-and-conquer strategy could be an alternative to avoid such difficulties. If we divide the whole flight time into intervals small enough to assume that the drag parameter and the gravitational acceleration be constant, then we can apply the analytic approaches to the rocket motion in each interval and obtain piecewise analytic solutions. The piecewise governing equation in the interval between $(n-1)$ and (n) states becomes

$$\frac{dv}{q^2 - v^2} = \frac{\bar{K}_n}{m}\frac{dm}{\dot{m}^*}, \tag{3.1.3a}$$

$$\dot{m}^* = \frac{m\bar{g}_n + \bar{K}_n q^2}{u_e}, \tag{3.1.3b}$$

$$\bar{K}_n = \frac{K_{n-1} + K_n}{2}, \qquad \bar{g}_n = \frac{g_{n-1} + g_n}{2} \tag{3.1.3c}$$

Integrating the right hand side of equation (3.1.3a) in the interval between $(n-1)$ and (n) states can be expressed as follows:

$$\int_{m_{n-1}}^{m_n} \frac{\bar{K}_n u_e}{m\bar{g}_n + \bar{K}_n q^2}\frac{dm}{m} = \frac{u_e}{q^2}\ln\left(\frac{m_n}{m_{n-1}}\frac{m_{n-1}\bar{g}_n + \bar{K}_n q^2}{m_n\bar{g}_n + \bar{K}_n q^2}\right). \tag{3.1.4a}$$

Hence, integrating equation (3.1.3a) from ground state to (n) state leads to

$$\frac{1}{2q}\ln\left(\frac{q + v_n}{q - v_n}\right) = \frac{u_e}{q^2}\sum_{i=1}^{n}\ln\left(\frac{m_i}{m_{i-1}}\frac{m_{i-1}\bar{g}_i + \bar{K}_i q^2}{m_i\bar{g}_i + \bar{K}_i q^2}\right). \tag{3.1.4b}$$

Rearranging this equation yields

$$v_n = q\frac{x_n - 1}{x_n + 1}, \tag{3.1.5a}$$

$$x_n = \left(\prod_{i=1}^{n} \frac{m_i}{m_{i-1}} \frac{m_{i-1}\bar{g}_n + \bar{K}_i q^2}{m_i \bar{g}_n + \bar{K}_i q^2}\right)^{\sigma} = \left(\prod_{i=1}^{n} \frac{m_i}{m_{i-1}} \frac{G_{i-1,i} + q^2}{G_{i,i} + q^2}\right)^{\sigma}, \tag{3.1.5b}$$

$$G_{i,j} = \frac{m_i \bar{g}_j}{\bar{K}_j}, \qquad \sigma = \frac{2u_e}{q}. \tag{3.1.5c}$$

The velocity parameter q is the limit of the velocity since the velocity approaches q as the variable x grows. The drag parameter and gravitational acceleration at the interval between $(n-1)$ and (n) states are not obtained until the velocity is determined. Thus it is necessary to calculate with iterations. The term x at the ground state and at the burn-out state become

$$x_o = \left(\frac{m_o}{m_o} \frac{G_{o,o} + q^2}{G_{o,o} + q^2}\right)^{\sigma} = 1, \tag{3.1.6a}$$

$$x_b = \left(\prod_{i=1}^{b} \frac{m_i}{m_{i-1}} \frac{G_{i-1,i} + q^2}{G_{i,i} + q^2}\right)^{\sigma}. \tag{3.1.6b}$$

The time derivative of mass flow rate between $(n-1)$ state and (n) state becomes

$$\frac{d\dot{m}^*}{dt} = \frac{\bar{g}_n}{u_e}\dot{m}^*, \quad \text{or} \tag{3.1.7a}$$

$$\frac{d\dot{m}^*}{\dot{m}^*} = \frac{\bar{g}_n}{u_e}dt. \tag{3.1.7b}$$

Integrating this equation between $(n-1)$ state and (n) state with inserting the mass flow rate expressed in equation (3.1.3b) yields

$$\ln \frac{m_n \bar{g}_n + \bar{K}_n q^2}{m_{n-1}\bar{g}_n + \bar{K}_n q^2} = \frac{\bar{g}_n}{u_e}(t_n - t_{n-1}). \tag{3.1.8a}$$

The mass can be expressed explicitly as follows:

$$m_n = \left(m_{n-1} + \frac{\bar{K}_n q^2}{\bar{g}_n}\right)\exp\left[\frac{\bar{g}_n}{u_e}(t_n - t_{n-1})\right] - \frac{\bar{K}_n q^2}{\bar{g}_n}. \tag{3.1.8b}$$

The rocket mass ratio and piecewise mass ratio between masses at $(n-1)$ and (n) states are defined as

$$\Omega = \frac{m_o}{m_b} > 1, \tag{3.1.9a}$$

$$\omega_n = \frac{m_{n-1}}{m_n} > 1. \tag{3.1.9b}$$

Also, the time can be represented as a function of mass as follows:

$$t_n - t_{n-1} = \frac{u_e}{\bar{g}_n}\ln\left(\frac{G_{n,n} + q^2}{G_{n-1,n} + q^2}\right). \tag{3.1.10}$$

The burn-out time can be determined with the summation of time intervals from ground state to burn-out state.

The altitude at burn-out state can be obtained by integrating the rocket velocity with respect to the time as follows:

$$h_b = \int_o^{t_b} v dt = \sum_{i=1}^{n} \int_{m_{i-1}}^{m_i} q\frac{x-1}{x+1}\frac{dm}{\dot{m}} = \sum_{i=1}^{n} \int_{m_{i-1}}^{m_i} q\frac{x-1}{x+1}\frac{u_e}{m\bar{g}_i + \bar{K}_i q^2}dm. \tag{3.1.11}$$

The altitude could not be integrated analytically even though the drag parameter and gravitational acceleration are constant in the piecewise intervals. In the present study, numerical integration with the Simpson rule [28] is used to obtain the altitude.

3.1.2. Solutions in coast phase

In coast phase, the governing equation cannot be analytically integrated since the drag parameter and gravitational acceleration are not constant. Hence we also have to apply the divide-and-conquer strategy. The differential of the altitude between $(n-1)$ state and (n) state can be expressed as follows:

$$dh = -m_b \frac{vdv}{m_b \bar{g}_n + \bar{K}_n v^2}. \tag{3.1.12a}$$

Integrating this equation between $(n-1)$ and (n) states yields

$$h_n - h_{n-1} = -\frac{m_b}{2}\frac{1}{\bar{K}_n}\ln\left(m_b\bar{g}_n + \bar{K}_n v^2\right)_{v_{n-1}}^{v_n} = \frac{m_b}{2}\frac{1}{\bar{K}_n}\ln\left(\frac{G_{b,n} + v_{n-1}^2}{G_{b,n} + v_n^2}\right). \tag{3.1.12b}$$

Then the altitude change from burn-out state to apogee becomes

$$h_{bs} = h_s - h_b = \frac{m_b}{2}\sum_{i=b+1}^{s}\frac{1}{\bar{K}_i}\ln\left(\frac{G_{b,i} + v_{i-1}^2}{G_{b,i} + v_i^2}\right). \tag{3.1.12c}$$

3.2. Optimal conditions at burn-out state

The rocket altitude changes according to the velocity parameter since the rocket velocity changes with the velocity parameter. We aim to find a way to determine the maximum altitude at burn-out state or at apogee for the flight in the standard atmosphere. The governing equation in boost phase can be rewritten according to the altitude instead of the time as follows:

$$\frac{dv}{q^2 - v^2} = \frac{K}{m}\frac{dh}{v}. \tag{3.2.1a}$$

Separating variables and integrating the above equation from ground state to burn-out state leads to

$$\int_o^{v_b} \frac{vdv}{q^2 - v^2} = \int_o^{h_b} \frac{K}{m}dh. \tag{3.2.1b}$$

The left side can be analytically integrated and is simply reduced as

$$-\frac{1}{2}\ln\left(\frac{q^2 - v_b^2}{q^2}\right) = -\frac{1}{2}\ln\left[\frac{4x_b}{(x_b+1)^2}\right]. \tag{3.2.2a}$$

Differentiating this term with respect to the velocity parameter yields

$$\left(-\frac{1}{2x_b} + \frac{1}{x_b+1}\right)\frac{dx_b}{dq} = \frac{1}{2x_b}\frac{x_b - 1}{x_b + 1}\frac{dx_b}{dq}. \tag{3.2.2b}$$

Differentiating the right hand side of equation (3.2.1b) with respect to the velocity parameter yields

$$\int_o^{h_b} \frac{d}{dq}\frac{K}{m}dh + \frac{K_b}{m_b}\frac{dh_b}{dq} - \frac{K_o}{m_o}\frac{dh_o}{dq}. \tag{3.2.3}$$

The Leibniz rule [29] is applied on the right hand side of equation (3.2.1b). The derivative of the altitude at ground state is zero. Also, for the maximum altitude, the derivative of the altitude at burn-out state should be zero. Thus the following characteristic equation must be satisfied for the maximum altitude at burn-out state.

$$\frac{1}{2x_b}\frac{x_b-1}{x_b+1}\frac{dx_b}{dq}=\int_o^{h_b}\frac{d}{dq}\frac{K}{m}dh. \tag{3.2.4}$$

Taking the logarithm of the term x_b expressed in equation (3.1.6b) yields

$$\ln(x_b)=\frac{2u_e}{q}\ln\left(\prod_{i=1}^{b}\frac{1}{\omega_i}\frac{G_{i-1,i}+q^2}{G_{i,i}+q^2}\right). \tag{3.2.5}$$

The parameter G changes with the velocity parameter due to the change of the altitude. But at the maximum altitude the derivative of the altitude becomes zero and thus we can ignore the derivative of the parameter G. Then differentiating this equation with respect to the velocity parameter yields

$$\frac{1}{x_b}\frac{\partial x_b}{\partial q}=-\frac{1}{q}\left[\ln(x_b)-4qu_e\sum_{i=1}^{b}\frac{G_{i,i}(1-\omega_i)}{(G_{i-1,i}+q^2)(G_{i,i}+q^2)}\right]. \tag{3.2.6}$$

Also, according to the same reason, we can ignore the derivative of the drag parameter on the right hand side of equation (3.2.4). Then applying the divide-and-conquer strategy leads to

$$-\sum_{i=1}^{b}\bar{K}_i\int_{h_{i-1}}^{h_i}\frac{1}{m^2}\frac{dm}{dq}dh. \tag{3.2.7a}$$

The mass at a given altitude would change with the velocity parameter and thus the derivative of the mass with respect to the velocity parameter could not vanish. As suggested in the previous study [23], the derivative of the mass with respect to the velocity parameter between $(n-1)$ and (n) states can be expressed as follows:

$$\frac{dm}{dq}=\frac{2q(m-\beta m_b)}{G_{n-1,n}+q^2}. \tag{3.2.7b}$$

If β is Ω, then the critical mass βm_b becomes m_o. The coefficient β would change with the rocket mass or rocket mass ratio.

Hence, the following characteristic equations should be satisfied to maximize altitude at burn-out state.

$$\ln(x_b)-4qu_e\sum_{i=1}^{b}\frac{G_{i,i}(1-\omega_i)}{(G_{i-1,i}+q^2)(G_{i,i}+q^2)}=S_b, \tag{3.2.8a}$$

$$S_b=\frac{x_b+1}{x_b-1}\sum_{i=1}^{b}\bar{K}_i\int_{h_{i-1}}^{h_i}\frac{4q^2}{G_{i-1,i}+q^2}\frac{m-\beta m_b}{m^2}dh. \tag{3.2.8b}$$

This equation is the fourth-order one but is impossible to be constructed in a polynomial form. Hence, to avoid this serious situation, it is inevitable to build alternative equation in a reduced order as follows:

$$q^3\left[\ln(x_b)-S_b\right]-4u_e\sum_{i=1}^{b}\frac{G_{i,i}(1-\omega_i)}{(\frac{G_{i-1,i}}{q^2}+1)(\frac{G_{i,i}}{q^2}+1)}=0,\quad \text{or} \tag{3.2.9a}$$

$$q\left[\ln(x_b)-S_b\right]-4u_e\sum_{i=1}^{b}\frac{G_{i,i}(1-\omega_i)}{(\frac{G_{i-1,i}}{q}+q)(\frac{G_{i,i}}{q}+q)}=0. \tag{3.2.9b}$$

The solution of the characteristic equation cannot be obtained analytically since the undetermined solution exists implicitly in the second term. Thus, we try to obtain the solution with the following iterative equation.

$$q_{k+1}=\sqrt[3]{\frac{4u_e}{\ln(x_{b,k})-S_{b,k}}\sum_{i=1}^{b}\frac{G_{i,i}(1-\omega_i)}{(\frac{G_{i-1,i}}{q_k^2}+1)(\frac{G_{i,i}}{q_k^2}+1)}},\quad \text{or} \tag{3.2.10a}$$

$$q_{k+1}=\frac{4u_e}{\ln(x_{b,k})-S_{b,k}}\sum_{i=1}^{b}\frac{G_{i,i}(1-\omega_i)}{(\frac{G_{i-1,i}}{q_k}+q_k)(\frac{G_{i,i}}{q_k}+q_k)}. \tag{3.2.10b}$$

Preliminary numerical experiments show that as same as the previous study [23], the first order approximation (3.2.10b) converges faster than the third order approximation (3.2.10a) and gives exactly same results. These equations are stable and, thus, converge within several iterations. The converged solution can be obtained within about 20 iterations that are slightly higher than that for the cases with constant drag parameter.

The term S_b in the above equation decreases and so does the estimated velocity parameter q_{k+1} as the coefficient β increases. Therefore, we can determine the coefficient β with the following iterative relation.

$$\beta_{k+1}=\beta_k\left[1-C_\beta\left(\frac{q}{h_b}\frac{dh_b}{dq}\right)_k\right]. \tag{3.2.11a}$$

On the contrary to the cases with a constant drag parameter considered in the previous study [23], the derivative of altitude with respect to the velocity parameter could not be explicitly determined since the drag parameter changes with the altitude that is not determined yet. A reasonable and simple alternative is numerical derivative represented as follows:

$$\frac{\partial h_b}{\partial q}\approx\frac{h_b(q+\Delta q)-h_b(q-\Delta q)}{2\Delta q}. \tag{3.2.11b}$$

The larger value of C_β in equation (3.2.11a) results in the faster convergence but the stronger instabilities. In the present study, the constant of 1/4 is used. On the other hand, the smaller Δq results in the more exact differentiation but the stronger instabilities. Preliminary numerical experiments showed that the difference of the velocity parameter Δq between 0.1% and 1.0% of the velocity parameter guaranteed stable convergences. In the present study, the difference of 0.5% is adopted.

3.3. Optimal conditions at apogee

The rocket in coast phase ascends until the apogee or apogee where the rocket velocity is zero. Hence, the optimal condition for maximizing altitude at apogee would differ from that at burn-out state. In coast phase, the thrust is terminated and the mass is constant. Thus, the governing equation becomes

$$-\frac{dv}{Kv^2+m_bg}=\frac{1}{m_b}\frac{dh}{v}. \tag{3.3.1a}$$

Separating variables yields

$$-\frac{Kvdv}{Kv^2+m_bg}=\frac{K}{m_b}dh. \tag{3.3.1b}$$

The left hand side of the above equation cannot be analytically integrated since the drag parameter is not constant. We can avoid such difficulty with the strategy of divide-and-conquer as applied to the burn-out situation. If we divide the whole flight time into intervals small enough to treat the drag parameter and gravitational acceleration as constants in each interval. Then the integral of the left hand side of the above equation in the interval between $(n-1)$ state and (n) state becomes

$$-\int_{v_{n-1}}^{v_n}\frac{\bar{K}_nvdv}{m_b\bar{g}_n+\bar{K}_nv^2}=\frac{1}{2}\ln\left(\frac{m_b\bar{g}_n+\bar{K}_nv_{n-1}^2}{m_b\bar{g}_n+\bar{K}_nv_n^2}\right). \tag{3.3.2}$$

The above term makes it difficult to analyze the behavior of the governing equation since we cannot determine the derivative of the intermittent velocities with respect to the velocity parameter. On the other hand, we can substitute the rocket velocity with another variable as follows:

$$w = \sqrt{K}v, \tag{3.3.3a}$$

$$dw = \sqrt{K}dv + \frac{v}{2\sqrt{K}}dK = \sqrt{K}v\left(\frac{dv}{v} + \frac{dK}{2K}\right). \tag{3.3.3b}$$

Both the velocity and the drag parameter have positive signs and negative rates and thus we can assume that the differentials have the following relationship:

$$\frac{dK}{K} = \psi\frac{dv}{v}. \tag{3.3.3c}$$

If the drag parameter changes in a similar mode, we assume that the ratio ψ is constant throughout the flight time in coast phase. The ratio ψ can be determined with comparing the drag parameters at burn-out state and at the state where the velocity is half of burn-out velocity as follows:

$$\psi = \frac{\ln[K(v_b)/K(v_b/2)]}{\ln(2)}. \tag{3.3.3d}$$

Hence the governing equation integrated from ground state to apogee approximately becomes

$$\int_o^{v_b}\frac{vdv}{q^2 - v^2} - \frac{2}{2+\psi}\int_{w_b}^{o}\frac{wdw}{w^2 + m_b g} = \int_o^{h_b}\frac{K}{m}dh + \int_{h_b}^{h_s}\frac{K}{m_b}dh. \tag{3.3.4}$$

The second term of the above equation is reduced as

$$-\frac{1}{2+\psi}\ln\left(\frac{m_b g_b}{m_b g_b + K_b v_b^2}\right) = \frac{1}{2+\psi}\ln\left(\frac{G_{b,b} + v_b^2}{G_{b,b}}\right), \tag{3.3.5a}$$

$$G_{b,b} = \frac{m_b g_b}{K_b}. \tag{3.3.5b}$$

The parameter G changes with the velocity parameter due to the altitude change. But at the maximum altitude the derivative of the altitude becomes zero and thus we can ignore the derivative of the parameter G. Differentiating the above term with respect to the velocity parameter yields

$$\frac{2}{2+\psi}\frac{v_b}{G_{b,b} + v_b^2}\frac{d}{dq}\left(q\frac{x_b - 1}{x_b + 1}\right) = \frac{2}{2+\psi}\frac{x_b - 1}{x_b + 1}\frac{q}{G_{b,b} + v_b^2}\left[\frac{x_b - 1}{x_b + 1} + \frac{2q}{(x_b+1)^2}\frac{dx_b}{dq}\right]. \tag{3.3.6}$$

On the other hand, differentiating the right hand side in equation (3.3.4) with respect to the velocity parameter leads to

$$\int_o^{h_b}\frac{d}{dq}\frac{K}{m}dh + \int_{h_b}^{h_s}\frac{d}{dq}\frac{K}{m_b}dh + \frac{K_b}{m_b}\frac{dh_b}{dq} - \frac{K_o}{m_o}\frac{dh_o}{dq} + \frac{K_s}{m_b}\frac{dh_s}{dq} - \frac{K_b}{m_b}\frac{dh_b}{dq}. \tag{3.3.7}$$

The Leibniz rule [29] is applied. The second and the last terms cancel out. The derivative of altitude at ground state is zero, and, for the maximum altitude, the derivative of altitude at apogee should be zero. The rocket mass after burn-out state is constant and thus its derivative is zero and, as mentioned in the above section, at the maximum altitude we can ignore the derivative of the drag parameter. Thus the second term vanishes but, as mentioned in the above section, the first term remains. Hence, the characteristic equation to indicate the optimal condition for maximizing altitude at apogee becomes

$$\frac{1}{x_b}\frac{dx_b}{dq} + \frac{4}{2+\psi}\frac{q}{G_{b,b} + v_b^2}\left[\frac{x_b - 1}{x_b + 1} + \frac{2qx_b}{(x_b+1)^2}\frac{1}{x_b}\frac{dx_b}{dq}\right] = 2\frac{x_b + 1}{x_b - 1}\sum_{i=1}^{b}\bar{K}_i\int_{h_{i-1}}^{h_i}\frac{1}{m^2}\frac{dm}{dq}dh. \tag{3.3.8a}$$

Rearranging this equation yields

$$\Gamma_b\frac{1}{x_b}\frac{dx_b}{dq} + \frac{4q}{2+\psi}\frac{x_b - 1}{x_b + 1} = 2\left(G_{b,b} + v_b^2\right)\frac{x_b + 1}{x_b - 1}\sum_{i=1}^{b}\bar{K}_i\int_{h_{i-1}}^{h_i}\frac{1}{m^2}\frac{dm}{dq}dh, \tag{3.3.8b}$$

$$\Gamma_b = G_{b,b} + q^2\left[1 - \frac{4\psi}{2+\psi}\frac{x_b}{(x_b+1)^2}\right]. \tag{3.3.8c}$$

Inserting equation (3.2.6) and equation (3.2.7) into the above equation leads to

$$\ln(x_b) - 4qu_e\sum_{i=1}^{b}\frac{G_{i,i}(1-\omega_i)}{(G_{i-1,i} + q^2)(G_{i,i} + q^2)} = S_s, \tag{3.3.9a}$$

$$S_s = \frac{4q^2}{(2+\psi)\Gamma_b}\frac{x_b - 1}{x_b + 1} + \frac{G_{b,b} + v_b^2}{\Gamma_b}\frac{x_b + 1}{x_b - 1} \times \sum_{i=1}^{b}\bar{K}_i\int_{h_{i-1}}^{h_i}\frac{4q^2}{G_{i-1,i} + q^2}\frac{m - m_{cr}}{m^2}dh. \tag{3.3.9b}$$

This equation is the fourth-order one but is impossible to be constructed in a polynomial form. Rearranging this equation yields a reduced order equation as follows:

$$q^3\left[\ln(x_b) - S_s\right] - 4u_e\sum_{i=1}^{b}\frac{G_{i,i}(1-\omega_i)}{(\frac{G_{i-1,i}}{q^2} + 1)(\frac{G_{i,i}}{q^2} + 1)} = 0, \quad \text{or} \tag{3.3.10a}$$

$$q\left[\ln(x_b) - S_s\right] - 4u_e\sum_{i=1}^{b}\frac{G_{i,i}(1-\omega_i)}{(\frac{G_{i-1,i}}{q} + q)(\frac{G_{i,i}}{q} + q)} = 0. \tag{3.3.10b}$$

The solution of the characteristic equation cannot be obtained analytically since the undetermined solution exists implicitly in the second term. Thus, we try to obtain the solution with the following iterative equation.

$$q_{k+1} = \sqrt[3]{\frac{4u_e}{\ln(x_{b,k}) - S_s}\sum_{i=1}^{b}\frac{G_{i,i}(1-\omega_i)}{(\frac{G_{i-1,i}}{q_k^2} + 1)(\frac{G_{i,i}}{q_k^2} + 1)}}, \quad \text{or} \tag{3.3.11a}$$

$$q_{k+1} = \frac{4u_e}{\ln(x_{b,k}) - S_s}\sum_{i=1}^{b}\frac{G_{i,i}(1-\omega_i)}{(\frac{G_{i-1,i}}{q_k} + q_k)(\frac{G_{i,i}}{q_k} + q_k)}. \tag{3.3.11b}$$

Preliminary numerical experiments show that the first order approximation (3.3.11b) converges faster than the third order one

Table 5.1
Standard atmosphere [30].

Layer	h (km)	T (K)	p (Pa)	Layer	h (km)	T (K)	p (Pa)
Troposphere	0	288.15	1.0133E+5		90	186.87	1.8359E−1
	11	216.77	2.2699E+4		100	195.88	3.2011E−2
Stratosphere	20	216.65	5.5293E+3	thermosphere	150	634.39	4.5422E−4
	32	228.49	8.8906E+2		200	854.36	8.4736E−5
	47	269.68	1.1585E+2		300	976.01	8.7704E−6
Mesosphere	51	270.65	7.0458E+1		400	995.83	1.4518E−6
	70	217.45	4.6342E+0		500	999.24	3.0236E−7
	85	188.89	4.4563E−1		600	999.85	8.2130E−8

(3.3.11a) and gives exactly same results, which is as same as the previous study [23]. However, in the case with a small mass ratio less than 1.5, the third order approximation shows more stable convergence. The converged solution can be obtained in 30 iterations that are almost same as that for the burn-out situation.

The term S_s in the above equation decreases and so does the estimated velocity parameter q_{k+1} as the coefficient β increases. Therefore, we can determine the coefficient β with iteration as follows:

$$\beta_{k+1} = \beta_k \left[1 - C_\beta \left(\frac{q}{h_s} \frac{dh_s}{dq} \right)_k \right], \tag{3.3.12a}$$

$$\frac{\partial h_s}{\partial q} \approx \frac{h_s(q+\Delta q) - h_s(q-\Delta q)}{2\Delta q}. \tag{3.3.12b}$$

The larger C_β in equation (3.3.12a) results in the faster convergence but the stronger instability. In the present study, the constant of 1/4 is used. On the other hand, the smaller Δq results in the more exact differentiation but the stronger instabilities. Preliminary numerical experiments showed that the difference of the velocity parameter Δq between 0.1% and 1.0% of the velocity parameter guaranteed stable convergences. In the present study, the same difference of 0.5% is adopted as the burn-out situation.

4. Numerical solutions

If the mass and velocity of the rocket are known at $(n-1)$, then the velocity at (n) can be obtained. The discretized governing equation becomes

$$m_{n-1/2} \frac{v_n - v_{n-1}}{\Delta t} = \dot{m}_{n-1/2} u_e - \bar{K}_n v_{n-1/2}^2 - m_{n-1/2} \bar{g}_n. \tag{4.1a}$$

$$\Delta t = t_n - t_{n-1} = \frac{u_e}{\bar{g}_n} \ln\left(\frac{m_n \bar{g}_n + \bar{K}_n q^2}{m_{n-1} \bar{g}_n + \bar{K}_n q^2} \right). \tag{4.1b}$$

The index $n-1/2$ denotes the average of a variable between $(n-1)$ and (n) states.

$$m_{n-1/2} = \frac{m_{n-1} + m_n}{2}, \tag{4.2a}$$

$$v_{n-1/2} = \frac{v_{n-1} + v_n}{2},$$

$$\dot{m}_{n-1/2} = \frac{\dot{m}_{n-1} + \dot{m}_n}{2} = \frac{(m_{n-1} + m_n)\bar{g}_n + 2\bar{K}_n q^2}{2u_e} \tag{4.2b}$$

The governing equation is then rewritten as follows:

$$m_{n-1/2} \frac{v_n - v_{n-1}}{\Delta t} = \dot{m}_{n-1/2} u_e - \frac{\bar{K}_n}{4} \left(v_{n-1}^2 + 2 v_{n-1} v_n + v_n^2 \right) - m_{n-1/2} \bar{g}_n. \tag{4.3a}$$

This discretized equation becomes a quadratic one as follows:

$$v_n^2 + 2\left(v_{n-1} + 2\frac{m_{n-1/2}}{\bar{K}_n \Delta t} \right) v_n + v_{n-1}^2 - \frac{4}{\bar{K}_n} \left(m_{n-1/2} \frac{v_{n-1}}{\Delta t} + \dot{m}_{n-1/2} u_e - m_{n-1/2} \bar{g}_n \right) = 0. \tag{4.3b}$$

This solution at (n) state is

$$v_n = -B + \sqrt{B^2 - C}, \tag{4.4a}$$

$$B = v_{n-1} + 2\frac{m_{n-1/2}}{\bar{K}_n \Delta t},$$

$$C = v_{n-1}^2 - \frac{4}{\bar{K}_n} \left(m_{n-1/2} \frac{v_{n-1}}{\Delta t} + \dot{m}_{n-1/2} u_e - m_{n-1/2} \bar{g}_n \right) \tag{4.4b}$$

In coast phase, the thrust term is extracted from the equations, and the mass is fixed as that at the burn-out state.

5. Calculation conditions

5.1. Atmosphere

The solution of the rocket equation depends strongly on the drag coefficient that varies with the ambient air density. Therefore, for the flight of a rocket in a real atmosphere, the density change according to altitude raises a critical issue for the rocket dynamics. In the present study, the density is determined according to the standard atmosphere [30] where the effects of wind, location or time are excluded. The standard atmosphere is composed of the troposphere, stratosphere, mesosphere, and thermosphere. The typical thermodynamic properties for the standard atmosphere are listed in Table 5.1.

There are no universal formulas to express the thermodynamic properties up to the very high altitude. So the piecewise continuous expression is adopted in the present study. For the standard atmosphere, the temperature in each layer is expressed as a linear function of the altitude. The temperature at an altitude between $(a-1)$ layer and (a) layer can be obtained as follows:

$$T = \frac{T_a - T_{a-1}}{h_a - h_{a-1}} (h - h_{a-1}) + T_{a-1}. \tag{5.1}$$

The pressure in each interval is expressed as an exponential function of the altitude. Then the pressure at an altitude between $(a-1)$ layer and (a) layer can be obtained as follows:

$$p = p_{a-1} \exp\left[\xi_a (h - h_{a-1}) \right], \tag{5.2a}$$

$$\xi_a = \frac{1}{h_a - h_{a-1}} \ln\left(\frac{p_a}{p_{a-1}} \right). \tag{5.2b}$$

We can then determine the density as a function of altitude with the thermodynamic state function for the ideal gas of air.

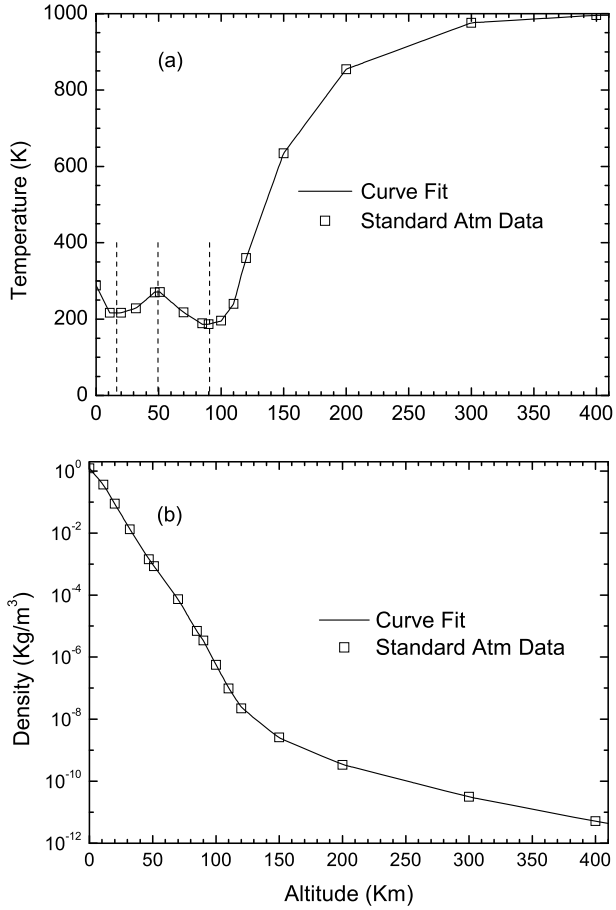

Fig. 1. Profile of thermodynamic properties according to altitude. (a) Variation of temperature according to the altitude and (b) Variation of density according to the altitude.

Table 5.2
Variations of rocket mass.

Dry mass (kg)	Total mass (kg)				
	$\Omega = 2$	$\Omega = 3$	$\Omega = 4$	$\Omega = 5$	$\Omega = 6$
500	1000	1500	2000	2500	3000
750	1500	2250	3000	3750	4500
1000	2000	3000	4000	5000	6000

Fig. 1 compares the changes of thermodynamic properties with altitude between data from the Standard Atmosphere [30] and that calculated with the functions used in the present study. The model function described in the above equations provides almost the same density as that of the Standard Atmosphere.

5.2. Rocket launching and propulsion conditions

In the present study, the absolute jet velocity at the nozzle exit is fixed as 1916 m/s. The rocket dry mass of 750 kg is considered. Also rocket dry masses of 500 kg and 1000 kg are considered for comparisons. The total mass or the propellant mass is determined according to the mass ratio, Ω. The mass ratio is varied from 2 to 6, which means the rocket total mass is changed from 1500 kg to 4500 kg. The conditions considered are listed in Table 5.2.

The cross-section diameter of the rocket is 0.6 m. The aerodynamic drag coefficient, C_d, is not a constant but a function of the Mach number. The basic model to simulate the effect of the Mach number is the one used by Ganji [18]. However the basic model showed some unstable behaviors near the Mach number of one.

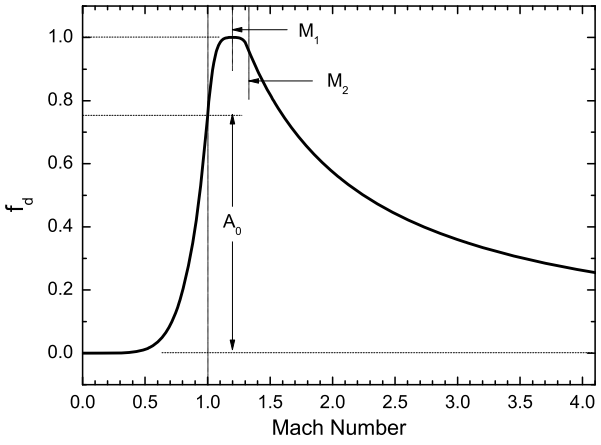

Fig. 2. Effect of Mach number on the factor f_d.

Hence, in the present study, the following model modified for the smooth transitions near the Mach number one is adopted.

$$C_d = C_{do}\left[1 + R_d f_d(M)\right], \tag{5.3a}$$

$$f_d(M) = \begin{cases} A_0 M^6, & M \le 1 \\ 1 - A_1(M - M_1)^4, & 1 < M \le M_2 \\ A_2(M + 1 - M_2)^{-1} & M_2 < M \end{cases}, \tag{5.3b}$$

$$A_1 = \frac{1 - A_0}{(M_1 - 1)^4}, \qquad A_2 = 1 - A_1(M_2 - M_1)^4. \tag{5.3c}$$

In the present study, the aerodynamic drag coefficient at ground state C_{do} and the jump ratio of the drag coefficient R_d are set as 0.8 and 1.1, respectively. The critical Mach numbers M_1 and M_2 in the above equation are set as 1.2 and 1.325, respectively. The coefficient A_0 is fixed as 0.75. Fig. 2 shows the Mach number effectiveness f_d on the aerodynamic drag coefficient.

5.3. Numerical approaches

If the number of piecewise intervals increases, the numerical solution or the piecewise analytic solution becomes more exact. Preliminary numerical experiment shows that in case the number of intervals for boost phase, N_b, is as great as 150, the numerical integration with the trapezoid rule yields almost the same result as that with the Simpson rule [28]. The number of piecewise intervals for boost phase and coast phase are fixed as 400 and 200, respectively. The mass change during each interval is assumed to be constant.

$$m_n - m_{n-1} = \frac{m_b - m_o}{N_b} = const. \tag{5.4}$$

For a numerical iteration in an interval, the iteration process is continued until the relative solution change is less than 10^{-7} of the solution.

6. Results

6.1. Solution profiles

Fig. 3 compares the velocity profiles between analytic and numerical solutions. The vertical dashed line indicates the burn-out time. The rocket velocities increase rapidly at early stage and after then keep constant until burn-out state. In coast phase, the velocities decrease due to the gravity force and aerodynamic drag. Fig. 3a shows the variations of velocity profile according to the rocket mass ratio with a fixed rocket mass of 750 kg. Regardless of the rocket mass ratio, each analytic solution is identical to the

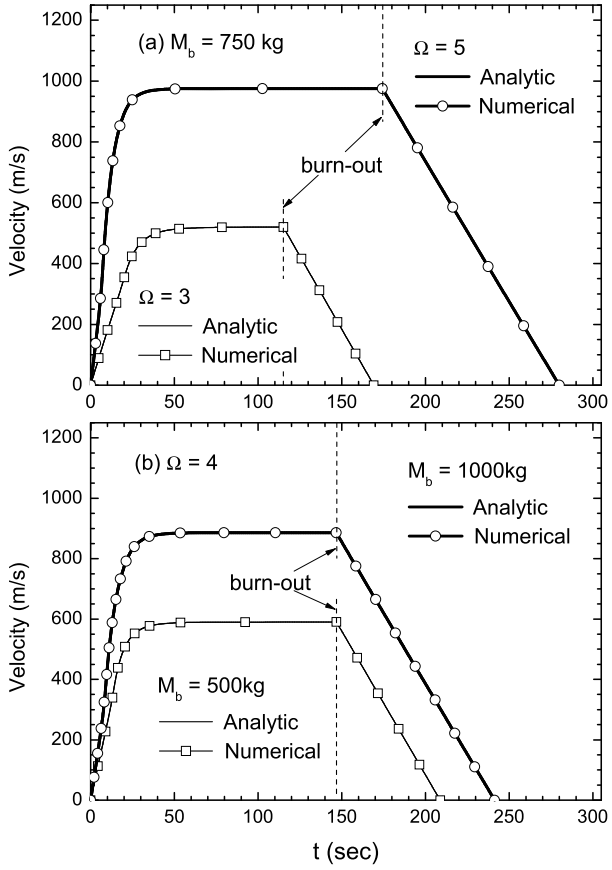

Fig. 3. Velocity profile according to time: (a) case with dry mass of 750 kg and (b) case with mass ration of 4.

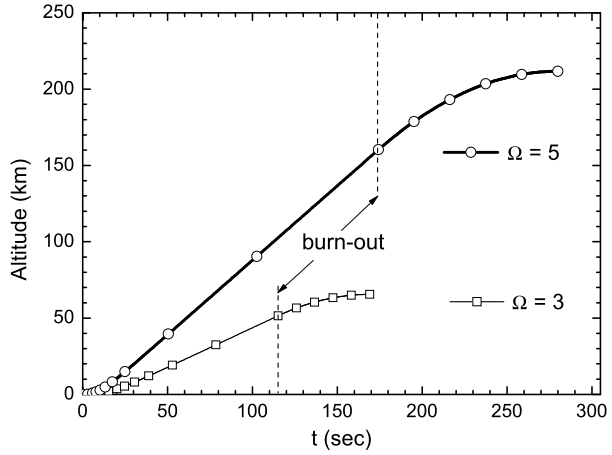

Fig. 4. Altitude profile according to time.

numerical one. The case with a higher mass ratio yields a higher rocket velocity and a longer time to apogee. Fig. 3b shows the variation of velocity profiles according to the rocket mass with a fixed rocket mass ratio of 4. Regardless of the rocket mass, each analytic solution is identical to the numerical one. The case with a higher mass yields a higher velocity but a similar time to apogee to the other.

Fig. 4 shows the changes of altitude with time. The rocket mass at burn-out state is 750 kg. The vertical dashed line indicates the burn-out time. In boost phase, the rocket altitude increases through concave curves at early stage and after then keeps constant slope until burn-out state. In coast phase, the rocket altitude

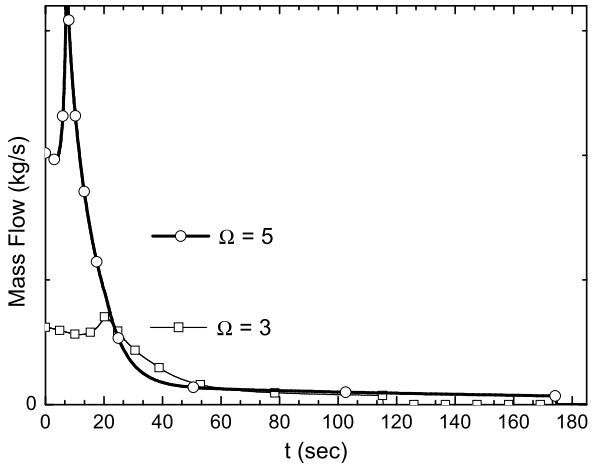

Fig. 5. Profiles of mass flow rate according to time.

changes through a convex curve, since the rocket is decelerated by gravity force. The increase of rocket mass ratio results in a increase of the maximum altitude.

Fig. 5 shows the profiles of mass flow rate according to time. The increase of mass ratio results in the proportional increase of the mass flow rate. For a given mass ratio, there are three distinctive regions. In the first region, the mass flow decreases gradually as the mass decreases. In the second region, the mass flow steeply increases and decreases because of the sharp increase and decrease of the drag coefficient where rocket passes the sonic barrier. In the third region, the mass flow decreases gradually with the decreases of the drag parameter and the rocket mass. The change of the mass flow rate is due to the constraint that the mass flow should be adjusted to keep the velocity parameter constant.

6.2. Optimal conditions at burn-out state

To determine the characteristic changes of the altitude at burn-out state according to the velocity parameter, the following normalized parameters are introduced.

$$\phi_b = \frac{q - q_{opt,b}}{q_{opt,b}}. \tag{6.1a}$$

$$\eta_b = \frac{h_b}{h_b(q_{opt,b})}. \tag{6.1b}$$

Fig. 6 shows the variations of the normalized altitude at burn-out state according to the normalized velocity parameter. The vertical dashed line indicates the optimal velocity parameter calculated by characteristic equation. The reduced order approximations of the characteristic equation (3.2.10) give the exact predictions of the optimal velocity parameter regardless of the rocket masses or the mass ratios. The values of the velocity parameter in the figure stand for the optimal ones at burn-out state where ϕ_b are zero. On the contrary to the previous study [23], the change of the normalized altitude on the right side is more sensitive to the velocity parameter than the other side, which is due to the drag reduction with altitude.

Fig. 6a represents the effects of the mass ratio on the variations of the normalized altitude. The case with the mass ratio of 2 seems much more sensitive to the velocity parameter than the other cases, which is due to that the rocket velocity is near to the speed of sound where the drag coefficient changes sensitively. Fig. 6b represents the effects of the rocket mass on the normalized rocket altitude. The normalized curves with different rocket masses nearly coincide even though the difference of the rocket

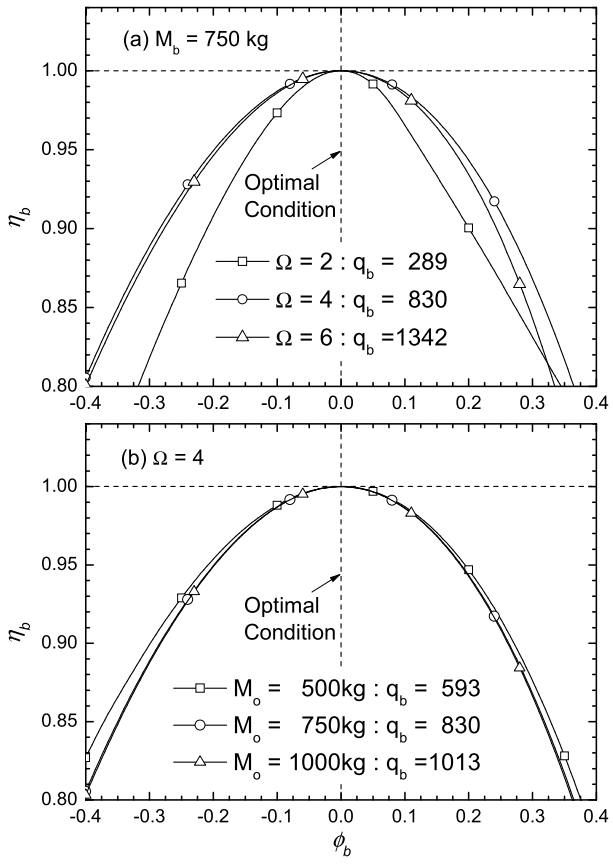

Fig. 6. Variation of altitude at burn-out state: (a) case with dry mass of 750 kg and (b) case with mass ration of 4.

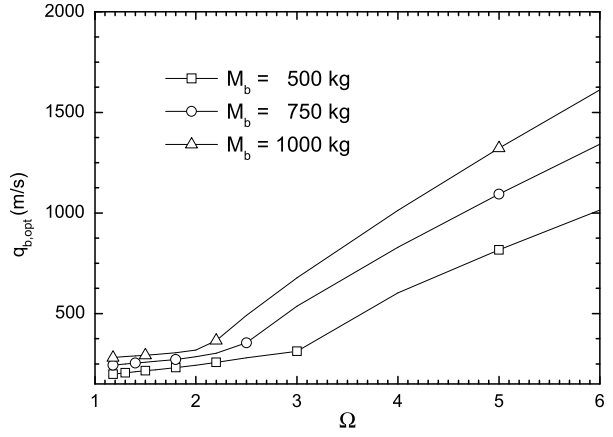

Fig. 7. Variation of optimal velocity parameters at burn-out state.

mass is remarkably large, which suggests that the variation of the normalized altitude is almost irrelevant to the rocket mass.

Fig. 7 shows variations of the optimal velocity parameters with the rocket mass or the rocket mass ratio at burn-out state. For a given rocket mass ratio, the optimal velocity parameter grows with the rocket mass but the growth rate slightly decreases as the rocket mass increases. For a given mass, there are two distinctive regions where the increasing rates of the optimal velocity parameter are very different. Regardless of the mass, the critical velocity parameter separating the regions is near to the speed of sound where the drag coefficient increases sensitively.

Fig. 8 shows variations of the maximum altitude at burn-out state with the rocket mass or the rocket mass ratio. For a given rocket mass ratio, the maximum altitude increases with the rocket

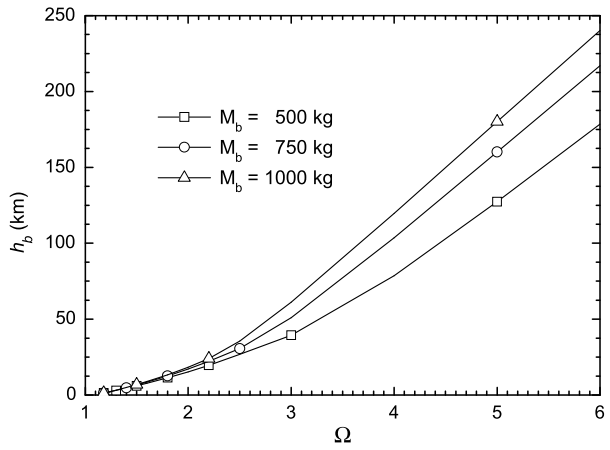

Fig. 8. Variation of maximum altitude at burn-out state.

mass but the rate slightly decreases as the rocket mass increases. For a given rocket mass, the altitude grows increasingly at lower mass ratio and after then grows with the mass ratio in a linear mode.

6.3. Optimal conditions at apogee

To determine the characteristic changes of altitude at apogee according to the velocity parameter, the following normalized parameters are introduced.

$$\phi_s = \frac{q - q_{opt,s}}{q_{opt,s}}. \tag{6.2a}$$

$$\eta_s = \frac{h_s}{h_s(q_{opt,s})}. \tag{6.2b}$$

Fig. 9 shows variations of the normalized altitude at apogee according to the normalized velocity parameter. The vertical dashed line indicates the optimal velocity parameter calculated by characteristic equation. The reduced order approximations of the characteristic equation (3.3.11) give the exact predictions of the optimal velocity parameter regardless of the rocket masses or mass ratios. The values of the velocity parameter in the figures stand for the optimal ones at apogee where ϕ_s are zero.

Fig. 9a represents the effects of the mass ratio on the altitude. The case with the mass ratio of 2 is much more sensitive on the left hand side but much less sensitive on the right hand side to the velocity parameter than the other cases. This is due to that the optimal velocity parameter is a little higher than the critical Mach number where the drag coefficient has the maximum value. Fig. 9b represents the effects of the rocket mass on the altitude. The normalized curves with different rocket masses nearly coincide even though the change of the rocket mass is remarkably large, which suggests that the variation of the normalized altitude is almost irrelevant to the rocket mass.

Fig. 10 shows the variations of the optimal velocity parameters with the rocket mass or the rocket mass ratio at apogee. For a given rocket mass ratio, the optimal velocity parameter grows with rocket mass. While, on the contrary to the situation at burn-out stare, for a given rocket mass, the optimal velocity parameter decreases steeply with the mass ratio until the minimum value and, after then, bounce back and grows gradually with the rocket mass ratio. For a given mass, there is distinctive region where the optimal velocity parameter is the minimum and maintained almost constant. The minimum velocity parameter is near to the speed of sound where the drag coefficient increases sensitively.

Fig. 11 shows variations of the maximum altitude at apogee with the rocket mass or the rocket mass ratio. For a given rocket

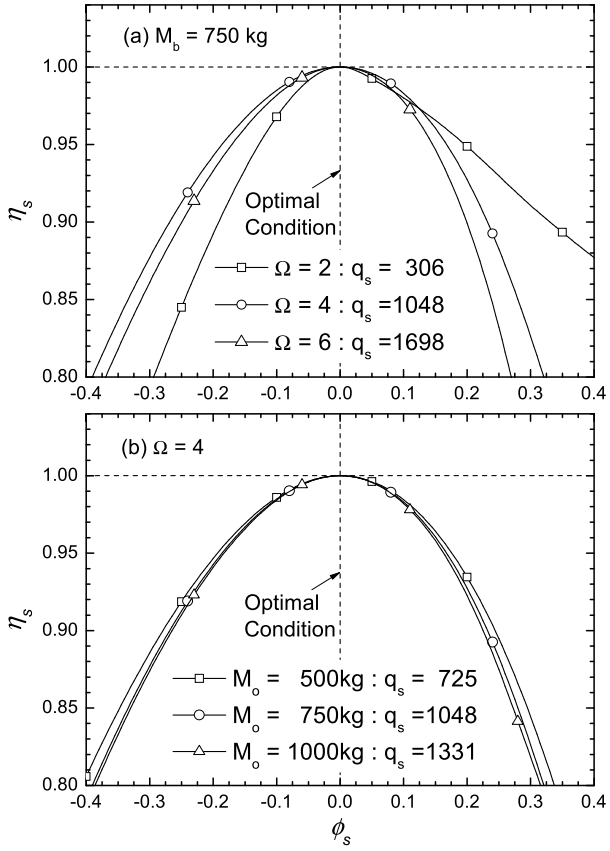

Fig. 9. Variation of altitude at apogee: (a) case with dry mass of 750 kg and (b) case with mass ration of 4.

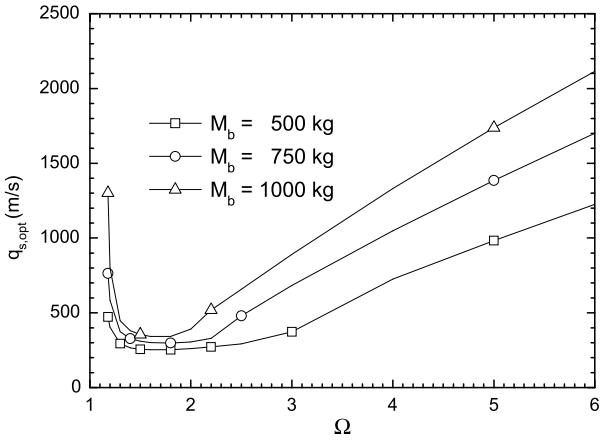

Fig. 10. Variation of optimal velocity parameters at apogee.

mass ratio, the maximum altitude increases with the rocket mass but the rate slightly decreases as the rocket mass increases. For a given rocket mass, the altitude grows increasingly at lower mass ratio and after then grows with the mass ratio in a linear mode.

7. Conclusions

The one-dimensional rocket momentum equation including thrust, gravitational force, and aerodynamic drag is examined to determine analytically the optimal condition for maximizing altitude of a sounding rocket at burn-out state or at apogee. The rocket flights in a standard atmosphere where the air density as well as the gravitational acceleration change with altitude are considered. Also the change of the aerodynamic drag coefficient with

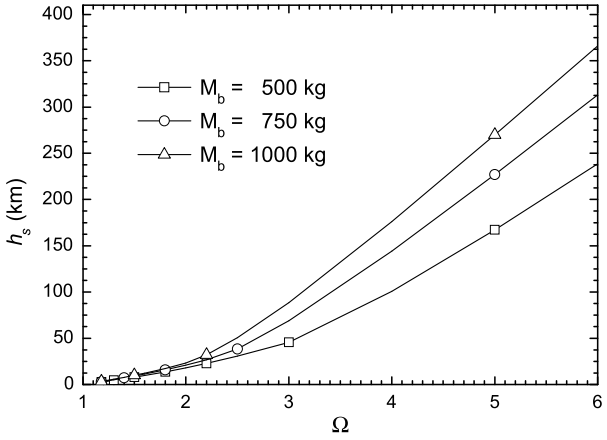

Fig. 11. Variation of maximum altitude at apogee.

the Mach number is considered. The piecewise analytic solutions are obtained with a divide-and-conquer strategy with which the whole flight time is divided into small intervals where the drag parameter and the gravitational acceleration can be treated as constants in each interval.

The piecewise analytic rocket velocity for a given velocity parameter can be obtained that matches the numerical one. For a given launching condition, there exists the optimal velocity parameter for maximizing altitude at burn-out state or at apogee. An analytic characteristic equation constructed from the analytic solution of the governing equation provides accurate predictions of the optimal conditions for maximizing altitude at burn-out state or apogee, which is confirmed by the numerical experiments.

In burn-out situation, the increase of the rocket mass at a given mass ratio results in the increases of the optimal velocity parameter but the increasing rate decreases as the rocket mass increases. The optimal velocity parameter at a given rocket mass grows with the rocket mass ratio in a linear mode. In apogee situation, the velocity parameter for maximizing altitude at apogee exists and is higher than that at the burn-out situation. Like the situation at burn-out state, the optimal velocity parameter grows with rocket mass, but there is the mass ratio where the optimal velocity parameter is the minimum at a given rocket mass, which is not shown in burn-out situation.

The present approach is restricted to the case where an analytic solution exists and thus does not provide the general solution of the classical Goddard problem. Because of the assumption that the mass flow of propellant should be adjusted to keep the velocity parameter constant, the application of the present results to a real problem would be limited. For instance, most of sounding rockets use the constant mass flow of propellant. But, unfortunately, the analytic solution of the problem does not exist. However, we could provide an approximate analytic solution of the problem with a proper modification of the present analytic approach. In the future study, we will search for alternative methods to get over the difficulties in dealing with the problem of constant mass flow. Adopting a new constant parameter that replaces the velocity parameter to guarantee analytic integration of the left hand side of equation (2.7), or exploiting piecewise analytic integrations with piecewise constant velocity parameters could be an alternative.

Conflict of interest statement

There is no conflict of interest.

Acknowledgements

This study was supported by the Special Research Fund for Mechanical Engineering in University of Ulsan.

References

[1] NASA sounding rocket program overview, http://rscience.gsfc.nasa.gov.
[2] S.F. Singer, Research in the upper atmosphere with high altitude sounding rockets, Vistas Astron. 2 (1) (1956) 878–912.
[3] G. Alford, G. Cooper, N. Peterson, Sounding rockets in Antarctica, in: 6th Sounding Rocket Conference, AIAA 1982-1754.
[4] M. Sanchez-Pena, Scientific experiences using Argentinean sounding rockets in Antarctica, Acta Astronaut. 47 (2000) 301–307.
[5] J.M. Grebowsky, D. Bilitza, Sounding rocket data base of E and D region ion composition, Adv. Space Res. 25 (1) (2000) 183–192.
[6] C.L. Croskey, J.D. Mitchell, M. Friedrich, K.M. Torkar, R.A. Goldberg, Charged particle measurements in the polar summer mesosphere obtained by DROPPS sounding rockets, Adv. Space Res. 28 (7) (2001) 1047–1052.
[7] S. Nakasuka, R. Funase, K. Nakada, N. Kaya, J.C. Mankins, Large membrane Furoshiki Satellite applied to phased array antenna and its sounding rocket experiment, Acta Astronaut. 58 (2006) 395–400.
[8] K. Dougherty, Upper atmospheric research at Woomera: the Australian-built sounding rockets, Acta Astronaut. 59 (2006) 54–67.
[9] G.-R. Cho, J.-J. Park, E.-S. Chung, S.-H. Hwang, The Korea Sounding rocket program, Acta Astronaut. 62 (2008) 706–714.
[10] P.J. Eberspeaker, D.D. Gregory, An overview of the NASA sounding rocket and balloon programs, in: 19th ESA Symposium on European Rocket and Balloon Programmes and Related Research, Bad Reichenhall, Germany, 7–11 June 2009.
[11] P. Sanz-Aranguez, J.S. Calero, Sounding rocket developments in Spain, Acta Astronaut. 64 (2009) 850–863.
[12] J.-S. Chern, B. Wu, Y.-S. Chen, A.-M. Wu, Suborbital and low-thermospheric experiments using sounding rockets in Taiwan, Acta Astronaut. 70 (2012) 159–164.
[13] J.M.C. Romero, Sounding rocket program in Peru, in: SpaceOps 2012 Conference, 2012-1275893.
[14] P.R. Richter, M. Lebert, H. Tahedl, D.-P. Hader, Physiological characterization of gravitaxis in Euglena gracilis and Astasia longa studies on sounding rocket flights, Adv. Space Res. 27 (5) (2001) 983–988.
[15] T. Vietoris, J.L. Elizey, P. Joulain, S.N. Mehta, J.L. Torero, Larminar diffusion flame in microgravity: the results of the Minitexus 6 sounding rocket experiment, Proc. Combust. Inst. 28 (2000) 2883–2889.
[16] A. Paull, H. Alesi, S. Anderson, HyShot Flight Program and how it was developed, AIAA 2002-4939.
[17] M.K. Smart, N.E. Hass, A. Paull, Flight data analysis of the HyShot 2 Scramjet flight experiment, AIAA J. 44 (10) (2006) 2366–2375.
[18] D.D. Ganji, M. Gorji, M. Hatami, A. Hasanpour, N. Khademzadeh, Propulsion and launching analysis of variable-mass rockets by analytical methods, Propuls. Power Res. 2 (3) (2013) 225–233.
[19] S.-H. Lee, Analytic approach to determine optimal conditions for maximizing altitude of sounding rocket, Aerosp. Sci. Technol. 40 (2015) 47–55.
[20] G. Leitmann, A calculus of variation of Goddard's problem, Acta Astronaut. 2 (1956) 55–62.
[21] P. Tsiotras, H. Kelley, Drag-law effects in the Goddard problem, Automatica 27 (3) (1991) 481–490.
[22] H. Seywald, E.M. Cliff, Goddard problem in presence of a dynamic pressure limit, J. Guid. Control Dyn. 16 (4) (1993) 776–781.
[23] K. Graichen, N. Petit, Solving the Goddard problem with thrust and dynamic pressure constraints using saturation functions, in: Proceedings of the 17th World Congress, The International Federation of Automatic Control, Seoul, July 6–11, 2008.
[24] G.P. Sutton, O. Biblarz, Rocket Propulsion Elements, 7th ed., John Wiley and Sons, 2001.
[25] Howard D. Curtis, Rocket vehicle dynamics, in: Orbital Mechanics for Engineering Student, 3rd ed., Elsevier Ltd., 2014, Chap. 11.
[26] Y. Chen, C. Wen, Z. Gong, M. Sun, Drag coefficient curve identification of projectiles from flight tests via optimal dynamic fitting, Control Eng. Pract. 5 (5) (1997) 627–636.
[27] G.G. Dutta, A. Singhal, A.K. Ghosh, Estimation of drag coefficient from flight data of a cargo shell, in: AIAA Atmospheric Flight Mechanics Conference and Exhibit, AIAA 2006-6149.
[28] S.D. Conte, C. de Boor, Elementary Numerical Analysis: An Algorithmic Approach, 3rd ed., McGraw Hill, 1988.
[29] F.B. Hildebrand, Advanced Calculus for Applications, 2nd ed., Prentice-Hall, 1976.
[30] US committee on Extension to the Standard Atmosphere, US Standard Atmosphere, NASA-TM-74335, 1976.